EFFECT OF TIM COMPRESSION LOADS ON BGA RELIABILITY

Nicholas Graziano[1], Harry Schoeller, Ph.D.[2] and Lars Bruno[3]

[1] Department of Mechanical Engineering, Binghamton University
NY, USA

[2] Universal Instruments Corporation
NY, USA

[3]Ericsson AB
Stockholm, Sweden
lars.bruno@ericsson.com

ABSTRACT
Compressive loads are often applied to Thermal Interface Materials (TIMs) to improve their thermal performance and this stress must be accommodated by the underlying solder joints. The effect of compressive loads on BGA reliability has been analyzed for SAC305 solder in thermal shock (-40/125 °C with 15 minutes dwells).

Assemblies were temperature cycled using two different simulated heat sinks with multiple load magnitudes. One delivered the load directly to the die while the other loaded the outer BGA rows through contact on the substrate. Die loaded samples were tested with and without a backplate. Additionally, two sets of samples were pre-aged for up to 1000 hours at 125 °C under compression prior to solder collapse measurements or thermal shock.

BGA thermomechanical reliability, under different loading configurations and magnitudes, was compared using Weibull failure rate distribution plots. Cross sectioning and dye and pry analyses were performed to identify the location and mode of failure. This work aims to provide guidance for the potential trade-offs between thermal performances and second level interconnect reliability.

Key words: TIM, compression, SAC 305, thermal reliability

INTRODUCTION
The continuing drive to get more computing power out of ever shrinking electronics has in turn driven the need for more efficient thermal solutions. Thermal Interface Materials (TIMs) are employed to aid in the dissipation of heat from a component to a heat sink by filling the gap between them with a highly conductive material. Often, the thermal resistance of the TIM can be further decreased by compressing the material to reduce the interface resistance. While compression is desired for improved thermal performance, the load is inevitably transferred to the solder joints bringing into question its effect on mechanical reliability.

Superimposed compression loads will alter the stress state experienced by the solder joints in typical reliability tests such as accelerated thermal cycling or vibration testing. This has the potential to alter the critical stress locations, both within the solder joint array as a whole as well as within the individual solder joints. This in turn can affect the failure locations and modes. One of the major concerns for reliability in electrical components is solder fatigue driven by CTE differences among the various materials being employed. Several studies have shown that added compressive loads can in fact slow failure due to solder fatigue and prolong the characteristic life of BGAs in accelerated thermal cycling [1,2].

While some previous work has examined TIM related loads before, this experiment hoped to take a closer look at some of the phenomena involved. Loads were distributed both over the bare die as well as around the perimeter of the substrate. In addition to this, samples were tested with and without a backplate to examine the effect of flexure. Lastly samples that were thermally pre-aged under compression were included as an accelerated study of shelf life. The creep collapse of the solder joints in high temperature storage has also been investigated in this study. This report will cover reliability in thermal shock testing between -40 °C and 125 °C with 15 minutes dwells at the temperature extremes.

EXPERIMENTAL
Test Vehicle
The test vehicle used in this experiment was a 29 mm × 29 mm bare die flip chip BGA with a 0.8 mm pitch, and 20 mil diameter SAC305 spheres. There were >1,200 I/Os comprising two daisy chain test nets. One chain monitored electrical continuity of the interior second level joints and one monitored the corners of the BGA array.

Up to nine components populated the eight-layer, 62 mil thick PCB in a 3×3 array. A Cu-OSP finish was used for

the pads and tooling holes were included to accommodate fixturing.
The boards were baked for three hours prior to being printed with a modern type 4, SAC305 solder paste. The components were then picked and placed on the board and reflow soldered at a peak temperature of 245 °C with roughly 60 seconds above the liquidus temperature.

Fixturing
Loads were delivered to the components individually by compressive fixtures as pictured in Figure 1. Each fixture consisted of a simulated heat sink compressed by four spring loaded bolts. Two different 45 mm × 45 mm heat sinks were machined from 4.76 mm thick aluminum. The first was a flat plate which delivered the load directly to the die (Figure 2a). The second had a cutout to accommodate the 680 µm thick die, instead loading around the edges of the substrate (Figure 2b). This was formulated as an extreme representation of loading over a lid or heat spreader. The first heatsink resulted in a contact area equal to the die area of 118 mm^2. The edge loaded heat sink contacted the substrate over the area of the outer three rows of the array resulting in a contact area of 303 mm^2.

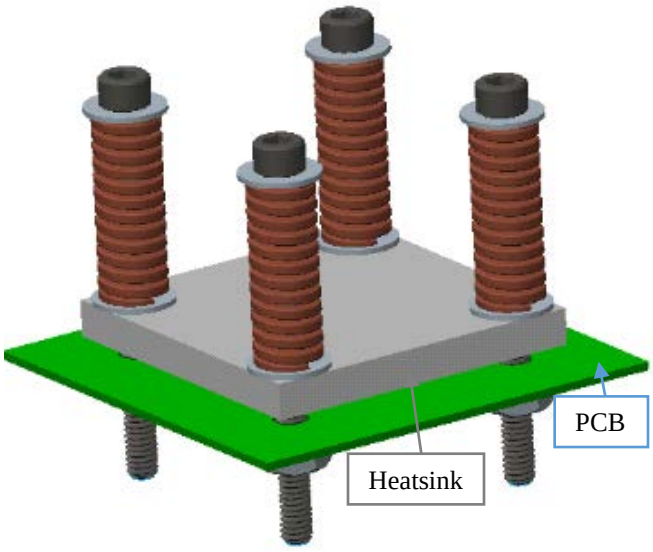

Figure 1. CAD generated image of compressive fixturing for an individual component.

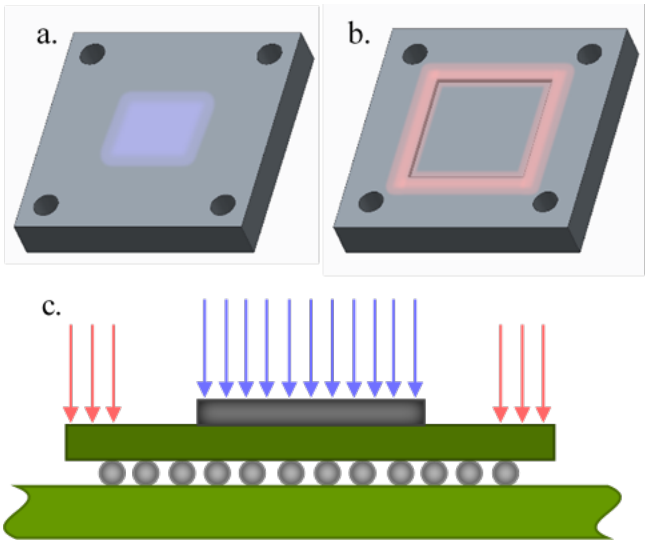

Figure 2. (a) Die loading heat sink, (b) edge loading heat sink, and (c) corresponding loading states on component.

Likewise, the PCB was constrained in two ways. Most samples were constrained with a 2.38 mm thick aluminum backplate. Alternatively, some samples were tested without a backplate instead supported only by washers on each bolt. These constituents were combined into the three different configurations pictured in Figure 3. The first configuration was loaded over the die and includes the backplate. The second configuration used the alternative heat sink in conjunction with the backplate to look at the effect of loading around the outside of the solder array. Lastly some samples were loaded over the die without the use of a backplate to consider the effect of additional flexure on reliability.

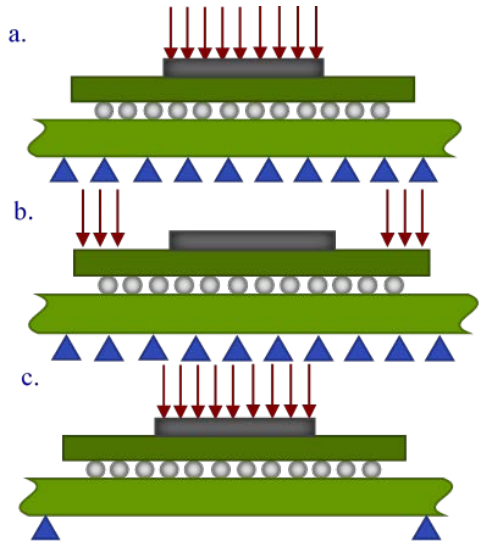

Figure 3. Compressive loading configurations subjected to thermal shock testing.

Discrete loads were determined based on percent compressions of a commercially available, high quality, TIM. Realistic assembly compressions of 30% and 50%

were chosen as well as an extreme case of 90%. Although an actual TIM was used in determining the necessary loads, one was not used in testing to avoid the complications of stress relaxation in the material. Rather, each die was coated with one layer of Kapton tape to act as a compliant buffer layer between the Si-die or substrate and the heat sink. The corresponding forces as well as the resulting pressures over the die and edge areas respectively have been tabulated in Table 1.

Table 1. Determined loads for desired percent compressions.

TIM Compression [%]	Initial Force [N]	Initial Pressure over Die [MPa]	Initial Pressure over Edge [MPa]
30%	17	0.15	0.06
50%	57	0.49	0.19
90%	587	4.97	1.94

Test Plan

Isothermal aging under compression was studied by first loading up samples to the desired TIM compression. The control was tested with fixturing in place, but no compression applied to maintain a similar thermal mass. The boards were then subjected to high temperature storage at 125 ˚C. Samples were taken out at regular intervals to be cross sectioned and measured. The test matrix is provided in Table 2.

Table 2. Isothermal aging test plan.

Test Condition	TIM Compression	Aging Time (hours at 125 ˚C)
(a)	0%	0, 250, 500, 1000
	30%	0, 250, 500, 1000
	50%	0, 250, 500, 1000
	90%	0, 250, 500, 1000

Thermo-mechanical reliability was measured using a thermal shock chamber. The test boards were cycled from -40 °C to 125 °C with 15 minutes dwells at the temperature extremes. The fixtures were assembled and samples were loaded up to the forces corresponding to the desired TIM compression. The control was tested with the fixturing in place but no compression applied to maintain a similar thermal mass. A total of 16 samples were tested for each of the conditions listed in Table 3.

Table 3. Thermal shock test plan.

Test Condition	TIM Compression	Pre-Aging (hours)
(a)	0%	-
	50%	0, 250, 500, 1000
	90%	-
(b)	0%, 50%, 90%	-
(c)	50%	-

Electrical continuity was monitored in-situ using an event detection system with an event designated as a momentary resistance above a threshold of 300Ω. Additionally, the boards were probed out manually at regular intervals. Initially the boards were probed every 200 cycles. After the first event, the duration was shortened to every 50 cycles. About 7% of the components were detected in this fashion. The 50 cycles' window gave a maximum possible error of 3% for time to failure. In addition, a few samples were occasionally unloaded to ensure that the pressure was not preventing failure detection by forcing cracks closed. The row at which each failure occurred was determined by probing the daisy chain net.

RESULTS

Thermal Shadow Moiré

Thermal shadow moiré was performed to characterize the component curvature over a simulated reflow profile. The warpage quantification and sign conventions used were in accordance with JEDEC Standard JESD22B11 [3]. Deflections were measured along the two diagonals and the curvature magnitude was defined by the average of the difference of the maximum and minimum deflections along both these axes. The component exhibited a convex curvature (edges down) at room temperature. Between 100 ˚C and 150 ˚C, the substrate reversed concavity and maintained a concave (edges up) curvature up to the maximum reflow temperature. In an actual reflow the solder would solidify around 200 ˚C locking the edges up orientation. The tendency of the substrate to revert to its original curvature at room temperature would thus result in unresolved stresses in the solder joints. Specifically, the joints near the edges would be in compression while the joints toward the center would be under a tensile stress. Component warpage over a simulated reflow profile is shown in Figure 4.

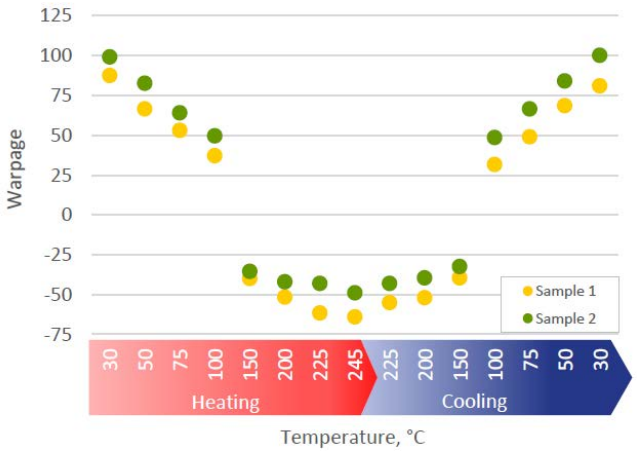

Figure 4. Component warpage over simulated reflow profile

Solder Collapse Due to Creep

In the isothermal aging test, the samples were stored for 100, 250, 500 and 1000 hours. In addition to this, time zero samples were loaded up to the proper compression at room

temperature, held for a minute, and then unloaded. The samples were cross sectioned to the center line of the component. Solder collapse was measured on joints at the very center and on the outside of the array.

The isothermal aging test resulted in BGA level solder joints having an average height of approximately 360 µm. The joint to joint variation was greater than the magnitude of collapse at every compression level up to 1000 hours, see Figure 5.

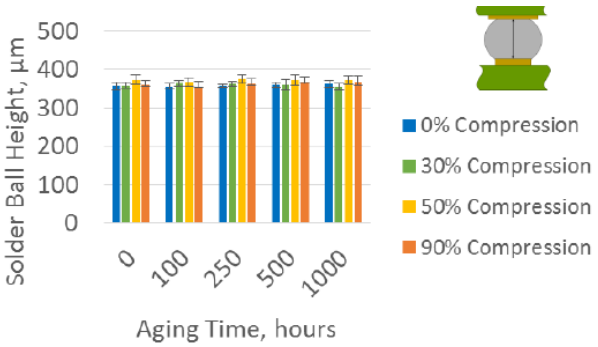

Figure 5. Average corner joint heights.

One trend that was noted was that the joints at the center of the component measured consistently shorter than those on the edges. This was consistent with the warpage observed in the shadow moiré analysis. However, the component warpage alone did not account for the fact that this height differential seemed to increase for the aged samples. An image that shows how the solder joint height differential is calculated is shown in Figure 6.

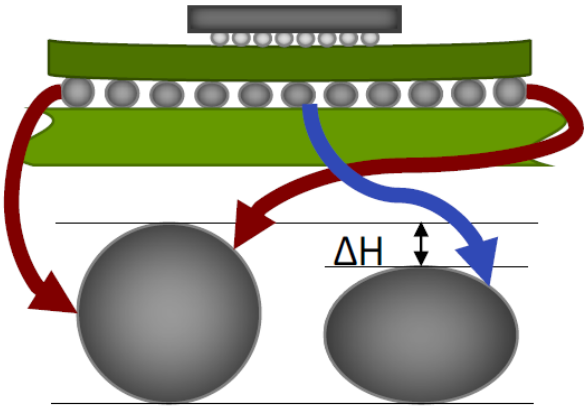

Figure 6. Solder joint height differential.

The height differential was quantified by averaging the heights of the two outside joints and subtracting out the height of the center joint for each sample. For the time zero samples, there was no obvious trend in the height differential. However, for the aged samples the differential appeared to increase with increasing load. This implies that the joints toward the center of the component collapsed at a faster rate which was consistent with the load distribution, where the load was delivered over the area of the die. Additionally, the stiffness of the substrate decreased at elevated temperatures, reducing its ability to distribute the load evenly to the solder array. These solder joint height differentials are shown in Figure 7.

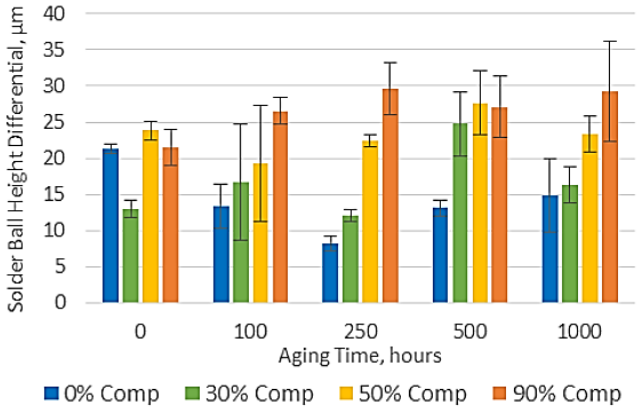

Figure 7. Solder joint height differential during aging.

The conclusion from the isothermal aging test is that solder collapse due to creep does not seem to be significant for the chosen compression loads.

Thermo-mechanical Reliability

Components were loaded under various configurations and magnitudes and tested in thermal shock from -40 °C to 125 °C with 15 minutes dwell at each extreme. Electrical continuity was measured in-situ and failures were confirmed by periodic manual probes.

Effect of Compression on Reliability

A Weibull failure rate distribution plot comparing the reliability of the edge loaded samples has been provided in Figure 8. The control sample had its first failure at 1407 cycles and produced a characteristic life of 1828 cycles. The sample with 50% loading around the edge of the substrate performed similarly with a first failure and characteristic life of 1500 and 1799 cycles, respectively. The extreme loading case, 90% around the edge, demonstrated more detrimental effects. It had the earliest first failure at 1325 cycles and a characteristic life of 1540 cycles; a 16% decrease relative to the control. All of the samples failed within 400 cycles of the first failure resulting in shape factors above 15 for each case. Further, the shape factors were all similar which suggests a common failure mode.

Loading the component over the die significantly changed the reliability of the component. The reliability data for the die loaded cases has been given in Figure 9. The control had its first failure at 1474 cycles and a characteristic life of 1814 cycles. The 50% die loading outperformed the control sample's characteristic life of 2437 cycles; a 34% increase in life. The 90% die loading performed even better with the highest characteristic life in the experiment at 2799 cycles. This represents a greater than 50% increase in lifetime over the unloaded control. While the control and moderate loading case distributions exhibited fairly constant slopes and shape factors above 15, the 90% loading case displayed

more variation. While the early failures occurred in quick succession, the Weibull slope leveled out about half way through the sample population. This resulted in a lower shape factor of around 8 and possibly indicates a change in failure mode.

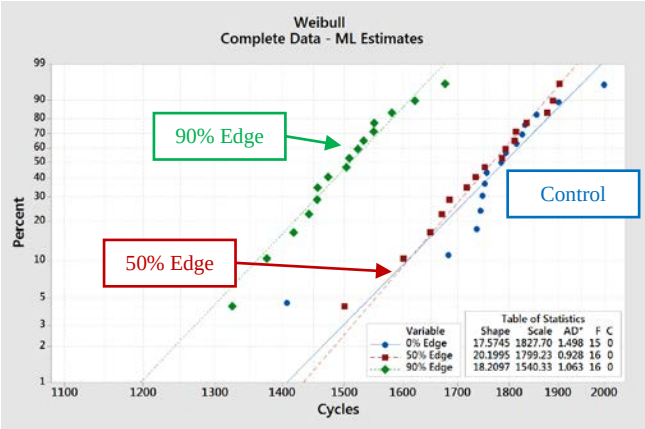

Figure 8. Weibull distribution plot comparing reliability of edge loaded samples.

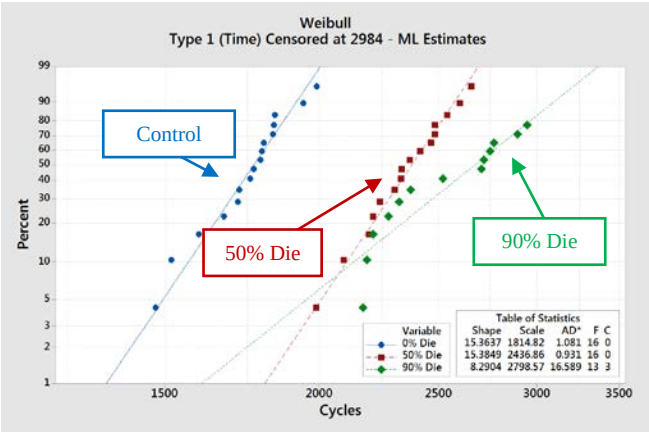

Figure 9. Weibull distribution plot comparing die loaded configurations.

In order to compare these different loading conditions, the extreme cases (90% TIM compression) for both the die and edge loading have been plotted in Figure 10. The two controls performed almost identically. This was to be expected as both were tested with fixturing in place, but no pressure applied. The case of 90% loading over the edge reduced the charac-teristic life while 90% loading over the die instead increased the characteristic life of the component. The die loaded case exhibiting an 82% increase in life over the edge loaded case.

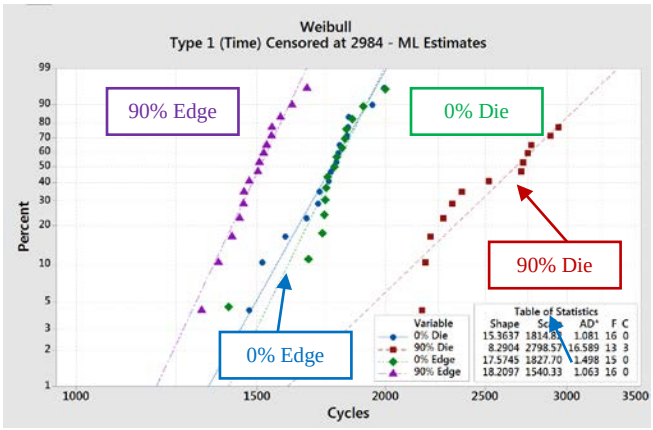

Figure 10. Weibull distribution plot comparing extreme loading cases.

Effect of Backplate on Reliability

As mentioned previously a subset of the 50% die loaded samples were tested without a backplate in place. The performance of this group has been compared to the 50% die loading with a backplate in Figure 11. It is clear that supporting the backside of the PCB has a positive effect on reliability. The no backplate case experienced its first failure about 100 cycles earlier at 1893 and ultimately yielded an inferior characteristic life of 2196 cycles, a 10% reduction. Despite this the slope of the graphs are nearly the same, indicative of a consistent failure mode.

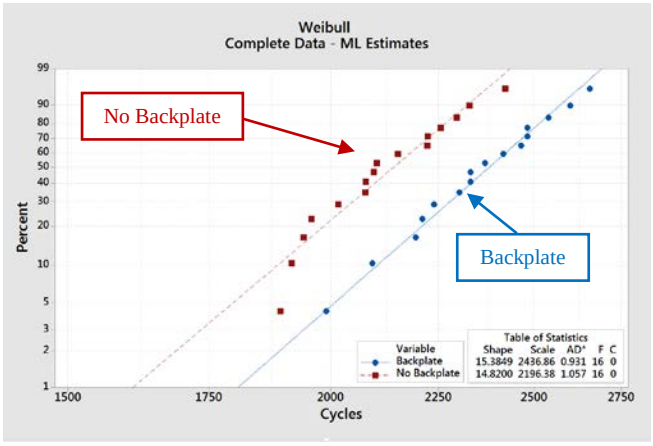

Figure 11. Weibull plot demonstrating effect of backplate on reliability.

Effect of Pre-aging on Reliability

Additionally, some of the 50% die loaded samples were pre-aged at 125 °C for 250, 500 or 1000 hours. As demonstrated in Figure 12, this did not appear to have a consistent effect on reliability. All of the samples had a first failure and characteristic life within 108 cycles, or 5%, of the unaged sample.

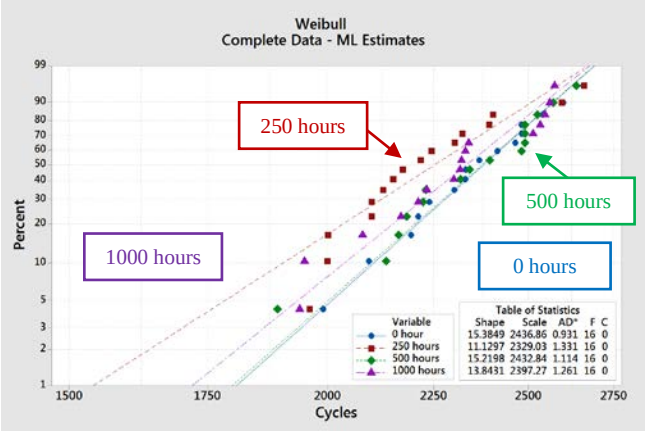

Figure 12. Weibull distribution plot demonstrating the effect of pre-aging on reliability.

Failure Analysis

Failure analysis was performed to better understand the failure locations and mechanisms at work. The BGA row of each failure was determined by hand probing the daisy chain net. Samples were then either cross-sectioned to the row of the failure or examined using dye-and-pry analysis. Cross-sectioning provides an ideal sample for microscopic analysis of individual solder joints whereas dye and pry allows one to view the extent of damage accumulated throughout the solder array.

The first two failures for each condition were removed; one was cross-sectioned while the other was used for dye and pry analysis. The remaining samples were left in the thermal shock chamber after failing to avoid drastically changing the thermal mass for the remaining components on the board. Many mid-life samples were later analyzed. Thus, both the cycles to failure and the cycles to removal will be noted to account for additional damage.

A representative control dye and pry sample is pictured in Figure 13 and Figure 14. The images are of the PCB side taken from above. Fatigue damage is indicated by the bright red dye within the interconnect areas. Not to be confused with the dye, the orange color visible is copper where joints were pulled out during the prying process. Silver color indicates solder damage from the prying process.

Damage appears to be concentrated heavily in the die shadow area. This is in accordance with the failure locations indicated by probing out the daisy chain. The inset image is a higher magnification image of the damaged area from a reduced angle. From this perspective it is clear that fatigue damage occurred near the component side of the solder joint.

A cross-polarizer micrograph of a cross-sectioned control sample is provided in Figure 15 to document the location of the crack within the solder joint. In accordance with the dye and pry analysis, the failure mode is solder fatigue near the component side pad. The crack appears to propagate intergranularly along recrystallized grain boundaries.

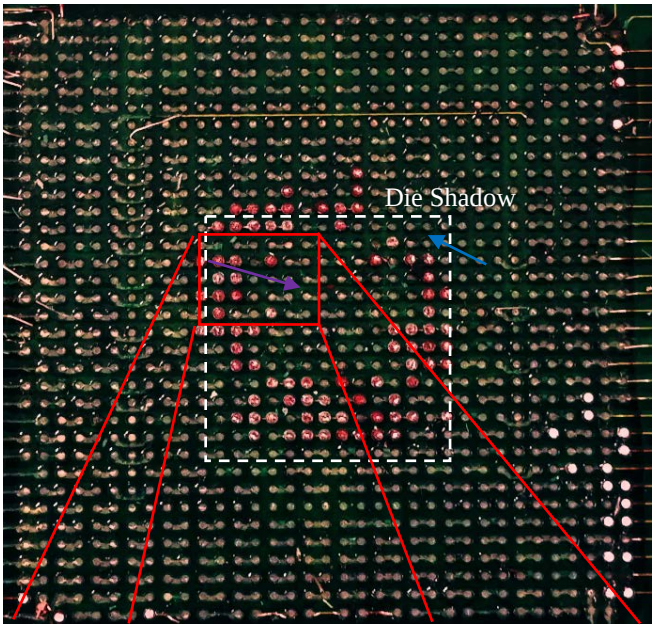

Figure 13. Unloaded control dye and pry (PCB side, failed: 1792 cycles, removed: 2021 cycles).

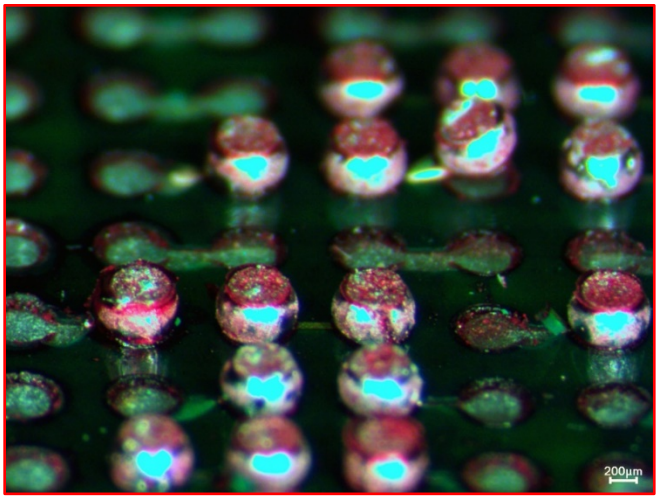

Figure14. Unloaded control dye and pry. This is the insert image, encircled in red, in Figure 13.

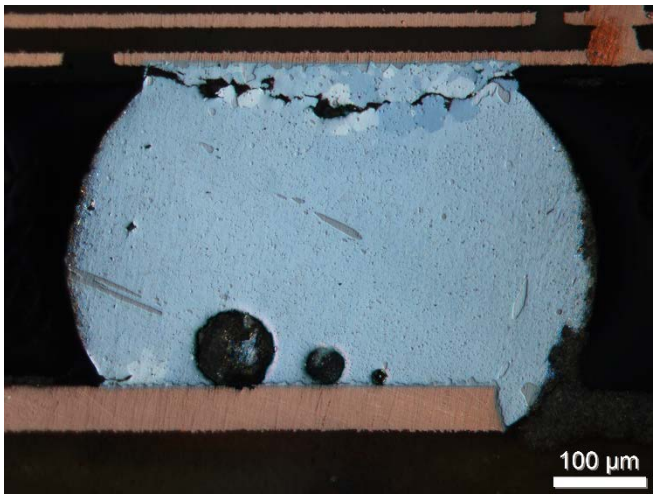

Figure 15. Failure mode in unloaded control sample is solder fatigue on component side. (186 u8).

This failure location and mode were consistent across all of the other loading conditions except for the 90% loading over the die. The Weibull distribution plot for this loading condition suggested a different failure mode. For this case event detection revealed that the corner daisy chain would often fail first. As corner joints are frequently non-functional, the parts were left in until the S-chain failed. Probing out the daisy chain by hand revealed that the corner joints had failed. This was confirmed by dye and pry analysis as displayed in Figure 16. Contrasting with the other loading configura-tions/magnitudes, Figure 13 and Figure 14 for example, this case yielded no damage in the die shadow region. Instead there is significant damage near the substrate corner. The inset image and the micrograph in Figure 17 reveal a consistent failure mode despite the change in location. While later samples demonstrated some damage under the die, failures remained component side, solder fatigue near the substrate edge.

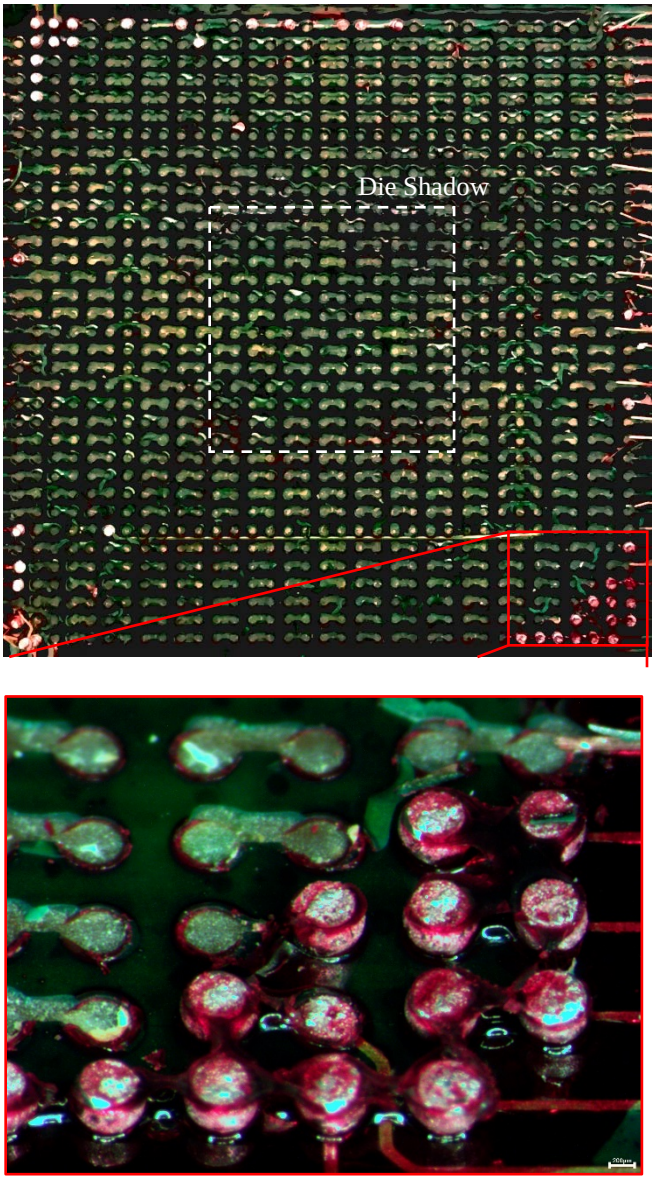

Figure 16. 90% die loaded failure, dye and pry analysis (PCB side, failed: 2146±25, removed: 2171).

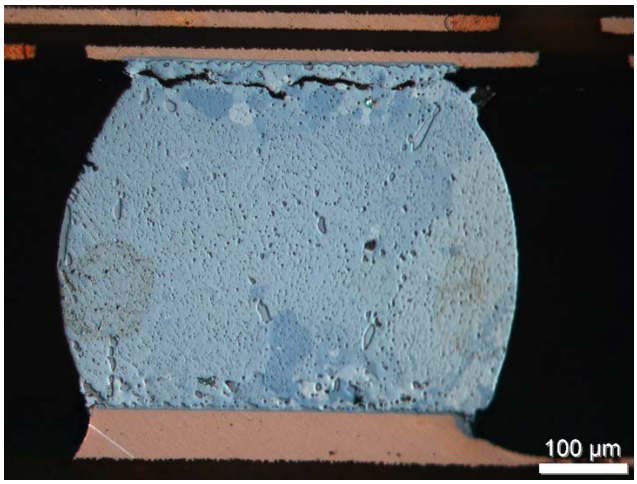

Figure 17. 90% die loaded cross-section (failed: 2186, removed: 2221).

DISCUSSION

Effect of Loading Distribution on Reliability

Loading over the die proved beneficial to thermo-mechanical fatigue life as previously reported by both Yu [1] and Chiu [2]. The realistic 50% loading over the die resulted in a 34% increase in the characteristic life. The extreme 90% loading case lasted 54% longer and failed near the edge of the substrate rather than under the die.

The critical stress region was revealed by the controls to be in the die shadow region. This failure location is common in BGAs due to the significant CTE mismatch between the die and the PCB [4]. As demonstrated by associated finite element modeling, the die loaded case resulted in a lower steady state plastic strain energy density increment per cycle at the critical joint. This indicates less damage accumulation as for instance in the Darveaux model [5]. Additionally, the superimposed compression in this region may have prolonged time to failure by forcing cracks closed and slowing their propagation as proposed by Chiu [2] and Bhatti [6].

Loading around the edge of the substrate did not yield the same effect. While the 50% edge loading displayed no discernable effect on reliability, the 90% loading proved detrimental. The modeling work similarly indicated a higher steady state plastic strain energy density increment per cycle at the critical location for the edge loading case. Additionally, modeling indicated a more tensile stress state under the die. This can expedite crack propagation by actively pulling cracks apart, opposed to compressive crack closure. This conclusion does not necessarily warrant concern, however. The 90% loading was being used as a non-realistic extreme. In practice a lid generally loads over the substrate in addition to the die rather than in lieu of it.

Change in Failure Location

Another consequence of the 90% die loading was a shift in failure location from the die shadow to the edge of the substrate. As mentioned previously, the die shadow is often the critical stress region due to CTE mismatches. The mismatch between the more similar materials that comprise the PCB and component substrate is generally not as significant.

Edge failures are instead driven by additional shear stresses due to component flexure. In order to quantify this flexure Shadow Moiré interferometry was performed on the unloaded PCB of the samples after testing. Tests were performed a day after the samples were unloaded, thus the flexure is due to plastic and inelastic deformation of the substrate. The deviations from planarity as defined by the JESD22-B112A [3] are plotted against the magnitude for the die loaded samples in Figure 18. Standard JESD22-B112A defines a negative or concave curvature as edges up. The control sample displays a slightly concave curvature as previously reported due to reflow. While the moderate loading over the die does not display a significant change in curvature, the 90% load yields about a 600% increase.

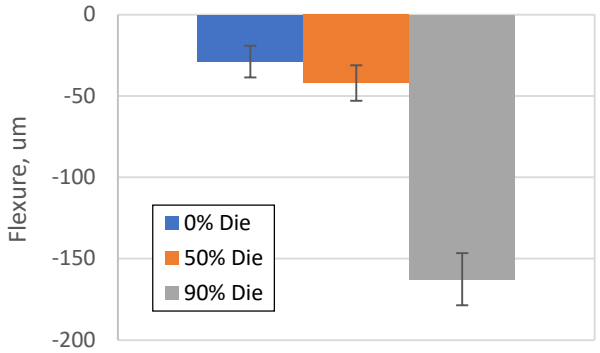

Figure 18. Flexure vs. TIM compression for die loading.

Thus, the additional flexure due to the die loading would result in compression under the die and tension near the edges of the component as indicated in Figure 19. Therefore, crack propagation may be suppressed in the die shadow region but assisted near the edge of the component.

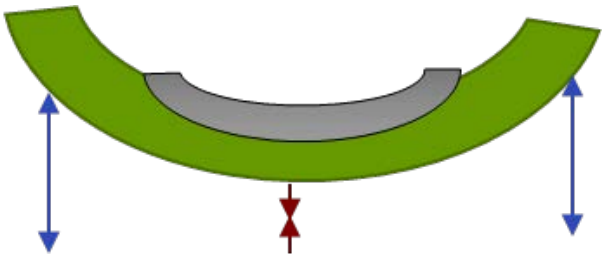

Figure 19. Resultant solder joint loading due to component substrate curvature.

As mentioned previously, the strain energy density per cycle is often correlated to fatigue damage in finite element analyses. The cyclic strain energy density for both the critical joint in the die shadow and at the component corner have been compared for the unloaded control and the 90% die loaded case in Figure 20. While the control model predicts slightly more damage at the corner than in the die

shadow region, the 90% die case was predicted to incur nearly six times as much damage at the component corner, which may explain the transition of the failure location to this region.

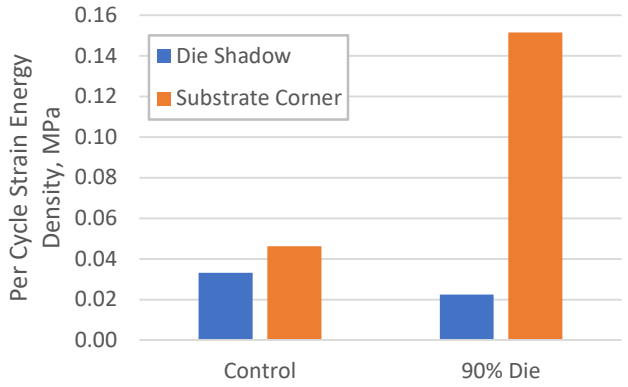

Figure 20. Plastic strain energy density per cycle at die shadow and substrate corner as determined by FEM.

Effect of Backplate

Assuming that a sample tested without a backplate is able to flex more freely, less of the compressive load will effectively be delivered to the solder joints. In order to quantify this effect, Shadow Moiré interferometry was performed on the back of the PCB for samples with and without the backplate with results shown in Figures 21 and 22, respectively. The no backplate case displayed significantly more warpage than the case with a backplate. The deviations from planarity as defined by the JESD22-B112A [6] were 146 µm and 40 µm, respectively.

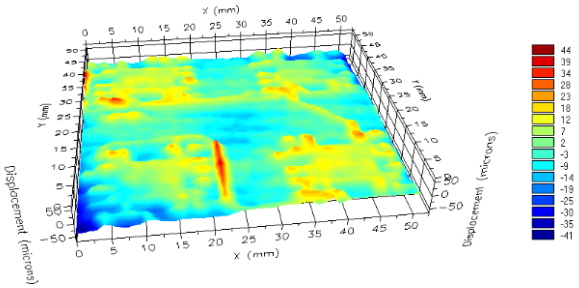

Figure 21. Shadow Moiré for 50% die loaded with backplate.

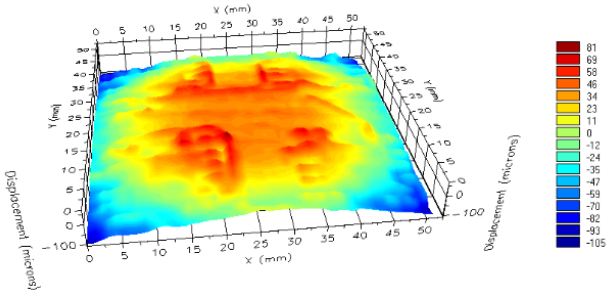

Figure 22. Shadow Moiré for 50% die loaded without backplate.

The stiffening effect of the backplate likely resulted in a more compressive stress state under the die. In contrast the flexural freedom in the unsupported case allowed the board to deflect away from the load. This was confirmed by extracting the average axial stress in the critical solder joint from the model which has been plotted in Figure 23. While the model supported by the backplate demonstrated a compressive stress throughout the solder ball in question, the unsupported case actually demonstrated a slightly tensile state. Thus, the unconstrained samples did not benefit from the crack suppressing effects of the superimposed compression.

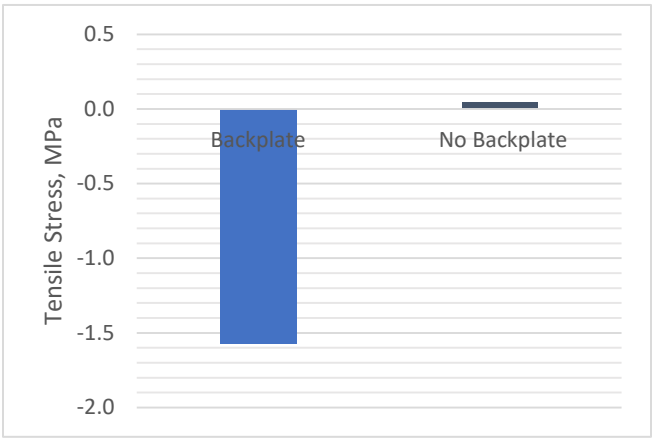

Figure 23. Average tensile stress for critical solder joint.

Effect of Pre-Aging

While pre-aging has been shown to have detrimental effects on the material properties of solder [7] this does not necessarily translate directly into a reduction in thermo-mechanical fatigue life. The pre-aged samples displayed little variation in reliability as illustrated in Figure 24. The characteristic life for each case is plotted while the error bars indicate the range of the first and last failure for each. These failure windows essentially overlap despite variation in the failure density within them.

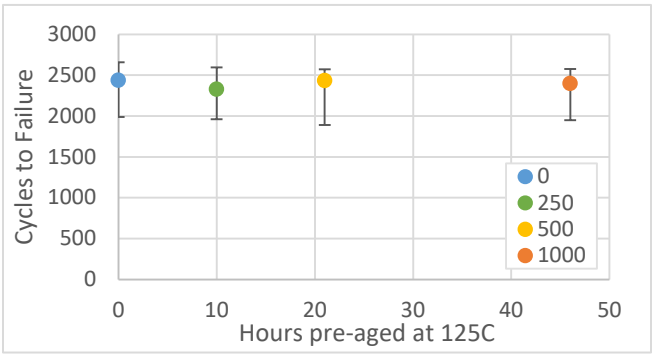

Figure 24. Reliability comparison for pre-aged samples.

A representative cross-polarized micrograph for the pre-aged samples has been provided in Figure 25. The failure mode remained intergranular fatigue cracks propagating through recrystallized grains near the component side pad.

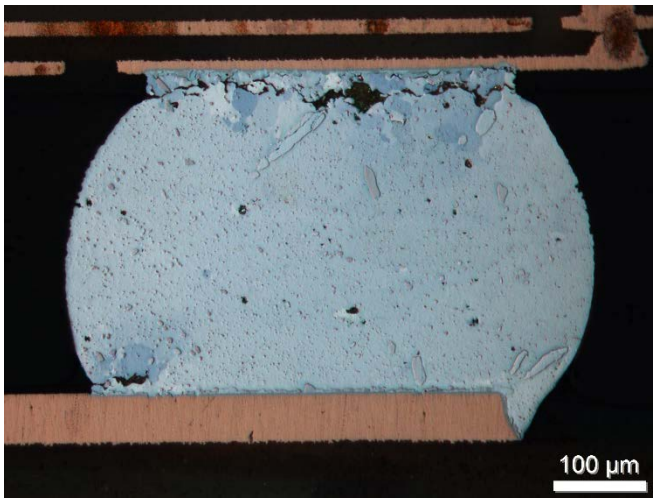

Figure 25. Cross-polarized micrograph of 1000 hour pre-aged sample (failed: 1938 cycles, removed: 1971 cycles).

As discussed previously in the isothermal aging portion of this experiment pre-aging resulted in coarsening of the Ag_3Sn precipitates [8]. Figure 26 compares the average precipitate size after various stages of testing. Pre-aging was performed for 1000 hours at 125 °C while thermal shock testing contributes about 2000 cycles of additional aging opportunity between -40 and 125 °C. While the pre-aged sample will presumably begin with larger precipitates, by the time failure occurs shock conditions will have contributed to precipitate coarsening as well. This resulted in a significant amount of variation within each condition and no statistically significant difference between them.

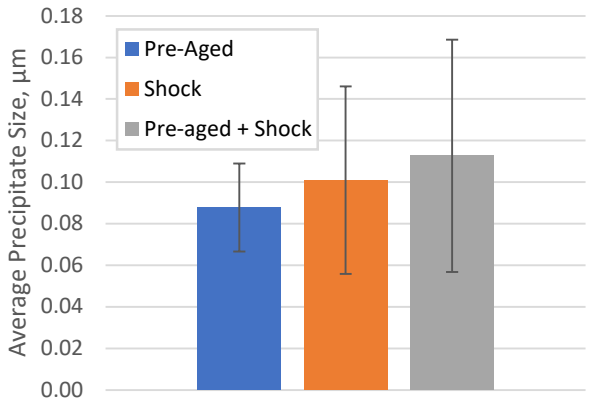

Figure 26. Ag_3Sn precipitate size for various test conditions.

CONCLUSIONS

TIM related compression loads have a significant effect on BGA reliability. They can lead to changes in both the time to failure as well as failure location.

The worst-case scenario was the 90% loading around the edge of the substrate. The 50% edge loading performed similarly to control case. Loading over the die had a positive effect on reliability. The 90% die loading was the best-case scenario. Using a backplate resulted in better performance by reducing flexure of the PCB. Pre-aging on the other hand had a negligible effect on reliability.

In addition to be the longest lasting sample, the 90% die loaded case was the only one that resulted in a different failure location. While the unloaded and all other cases failed in the die shadow, the 90% die loaded failed instead near the edge of the substrate. Regardless of the location, the failure mode was found to be solder fatigue near the component side pad.

ACKNOWLEDGEMENTS

The authors gratefully acknowledge the AREA Consortium and its member companies for supporting this study, with special thanks to Michael Meilunas and Jim Wilcox of Universal Instruments and Anne-Kathrine Knoph, Bo Eriksson, Christofer Markou, Benny Gustafson and Vilim Milotic of Ericsson AB.

REFERENCES

1. Yu, Da, Hohyung Lee, and Seungbae Park. "Reliability Assessment of Preloaded Solder Joint under Thermal Cycling." *Journal of Electronic Packaging* 134, no. 4 (2012): 041008.
2. Chiu, Tz-Cheng, Darvin Edwards, and Mudasir Ahmad. "Ball Grid Array Solder Joint Reliability Under System-Level Compressive Load." *IEEE Transactions on Device and Materials Reliability* 10, no. 3 (2010): 324-37.
3. JESD-B112A, “Package Warpage Measurement of Surface-Mount Integrated Circuits at Elevated Temperature” JEDEC Solid State Technology Association, 2009.
4. Garner, Luke, Charles Zhang, Keh Shin Beh, Kayleen Helms, and Yew Lip Tan. "Effect of compression loads on the solder joint reliability of flip chip BGA packages." In *Electronic Components and Technology Conference, 2004. Proceedings. 54th*, vol. 1, pp. 692-698. IEEE, 2004.
5. Darveaux, Robert. "Effect of simulation methodology on solder joint crack growth correlation and fatigue life prediction." *Journal of Electronic Packaging*124, no. 3 (2002): 147-154.
6. Bhatti, Pardeep K., Min Pei, and Xuejun Fan. "Reliability analysis of SnPb and SnAgCu solder joints in FC-BGA packages with thermal enabling preload." In*Electronic Components and Technology Conference, 2006. Proceedings. 56th*, pp. 6-pp. IEEE, 2006.
7. Suhling, Jeffrey C., Yifei Zhang, Zijie Cai, and Pradeep Lall. "Aging Effects on the Mechanical Behavior and Reliability of SAC Alloys." In *ASME 2009 InterPACK Conference collocated with the ASME 2009 Summer Heat Transfer Conference and the ASME 2009 3rd International Conference on Energy Sustainability*, pp. 959-976. American Society of Mechanical Engineers, 2009.

8. Lee, Tae-Kyu, and Hongtao Ma. "Aging impact on the accelerated thermal cycling performance of lead-free BGA solder joints in various stress conditions." In *Electronic Components and Technology Conference (ECTC), 2012 IEEE 62nd*, pp. 477-482. IEEE, 2012.